Seakeeping time domain simulations for surf-riding/broaching: investigations toward a direct stability assessment

P. Gualeni, D. Paolobello, N. Petacco & C. Lena

Journal of Marine Science and Technology
Official Journal of the Japan Society of Naval Architects and Ocean Engineers (JASNAOE)

ISSN 0948-4280

J Mar Sci Technol
DOI 10.1007/s00773-020-00704-x

Springer

Your article is protected by copyright and all rights are held exclusively by The Japan Society of Naval Architects and Ocean Engineers (JASNAOE). This e-offprint is for personal use only and shall not be self-archived in electronic repositories. If you wish to self-archive your article, please use the accepted manuscript version for posting on your own website. You may further deposit the accepted manuscript version in any repository, provided it is only made publicly available 12 months after official publication or later and provided acknowledgement is given to the original source of publication and a link is inserted to the published article on Springer's website. The link must be accompanied by the following text: "The final publication is available at link.springer.com".

Author's personal copy

Journal of Marine Science and Technology
https://doi.org/10.1007/s00773-020-00704-x

ORIGINAL ARTICLE

Seakeeping time domain simulations for surf-riding/broaching: investigations toward a direct stability assessment

P. Gualeni[1] · D. Paolobello[1] · N. Petacco[1] · C. Lena[2]

Received: 6 August 2019 / Accepted: 29 January 2020
© The Japan Society of Naval Architects and Ocean Engineers (JASNAOE) 2020

Abstract
Seakeeping time domain simulations are carried out to capture the likelihood of a surf-riding and/or broaching event, with the aim to gain a further insight into the ship performance in stern quartering seas. The applied numerical tool, named PANSHIP, is a 6-DoFs time domain seakeeping software based on panel method, combined with semi empirical viscous models. The investigated ships are two yacht vessels and a patrol boat. Calculations are also carried out with a tool implementing the IMO second level vulnerability criterion for surf-riding/broaching. Similarities, differences and critical issues of both approaches are discussed, as a first step in the perspective of a comprehensive application of the IMO Second Generation Intact Stability criteria, inclusive of the so-called "Direct Stability Assessment".

Keywords Surf-riding · Broaching · Second generation intact stability criteria · Direct stability assessment

1 Introduction

During the sixth session of the IMO Sub-Committee on Ship Design and Construction (SDC), the Second Generation Intact Stability (SGIS) criteria have been finalized [1]. As a framework for the criteria, a multi-layered approach has been adopted, with three assessment levels of increasing accuracy.

The stability failure modes taken into account within the SGIS criteria are: pure loss of stability, parametric roll, dead ship condition, surf-riding/broaching and excessive accelerations.

The broaching phenomenon could be included among the addressed stability failure modes relying on the extensive investigation activity developed during the recent decades, based on experimental tank tests [2, 3] as well as on numerical simulations [4].

In literature, the link between broaching and the surf-riding phenomenon has been recognized [5, 6]. Broaching is defined as a violent uncontrollable turning event that occurs despite maximum steering efforts to maintain course. It is accompanied by a large heel angle, which has the potential effect of a partial or total stability failure.

The surf-riding phenomenon occurs when a wave reaches a ship from the stern and accelerates her to wave celerity. In this condition, ships may be affected by directional instability leading to broaching. An in-depth study about the physics of these phenomena is given also in [7].

Since surf-riding precedes broaching, in the context of SGIS criteria, the evaluation of the likelihood for surf-riding occurrence has been assumed as a valuable information to assess the ship attitude to broaching. To this regard, a mathematical approach to solve a 1-DoF non-linear problem regarding longitudinal forces has been adopted in the second level of the criterion.

It is implied that because of the unidirectional nature of the adopted model, the broaching phenomenon cannot by any means be captured and described in such a way. Nevertheless, the broaching failure mode could be more properly analyzed by means of a more comprehensive numerical tool, in a direct stability assessment perspective, meant as a further (third) level of SGIS criterion.

In this paper, a useful tool able to perform a numerical simulation in time-domain is selected and a methodology to identify both surf-riding and broaching phenomena is presented. The outcomes have been compared with those obtained by the application of the Level 2 of SGIS criterion, which deals with the Surf-riding issue as mentioned above and detailed in the following.

✉ P. Gualeni
paola.gualeni@unige.it

[1] University of Genoa, Genoa, Italy

[2] Seakeeping Department, MARIN, Wageningen, The Netherlands

Published online: 12 February 2020

Author's personal copy

In relation with the significant differences between the two approaches, an overview of the issues related to their different physical background and comments on the comparability of the results are given.

2 The numerical tool

PANSHIP is based on a panel method that accounts for the free surface through the transient free surface Green function [8]. Two Cartesian axis systems are used. A ship-fixed axis system (x, y, z) with its origin in the ship's centre of gravity and a space-fixed axis system (x_0, y_0, z_0) with its origin in the undisturbed water surface and the z_0 axis pointing upwards. The ship-fixed axis system is fixed to the centre of gravity as already mentioned and rotates with the ship. The x-axis points to the bow, the y-axis points to port and the z-axis points upwards. The vessel is considered to be a rigid body. By using Newton's second law, and a suitable angular orientation vector (φ, θ, ψ), expressing the craft's orientation relative to the space-fixed axis system, the basic so-called Euler equations of motion are defined in Eq. 1, in a ship-fixed axis system:

$$\begin{cases} m\left(\dot{u} + \dot{\theta} \cdot w - \dot{\psi} \cdot v\right) = X - mg \cdot \sin\theta \\ m(\dot{v} + \dot{\psi} \cdot y - \dot{\varphi} \cdot w) = Y - mg \cdot \cos\theta \cdot \sin\varphi \\ m\left(\dot{w} + \dot{\varphi} \cdot v - \dot{\theta} \cdot u\right) = Z - mg \cdot \sin\theta \cdot \cos\varphi \\ \ddot{\varphi} \cdot I_{xx} + \theta \cdot \psi\left(I_{zz} - I_{yy}\right) = K \\ \ddot{\theta} \cdot I_{yy} + \psi \cdot \varphi\left(I_{xx} - I_{zz}\right) = M \\ \ddot{\psi} \cdot I_{zz} + \varphi \cdot \theta\left(I_{yy} - I_{xx}\right) = N \end{cases} \tag{1}$$

where X, Y and Z denote the force components and K, M and N denote the moment components acting on the craft. The translational velocity vector is given by (u, v, w) and the angular velocity vector is $(\dot{\varphi}, \dot{\theta}, \dot{\psi})$. The mg terms represent the gravity forces acting on the craft. The mass moments of inertia I_{xx}, I_{yy} and I_{zz} are constant in the ship-fixed axis system. An overdot denotes differentiation with respect to time.

The time derivative of the angular orientation vector (φ, θ, ψ) may be expressed in the angular velocity vector $(\dot{\varphi}, \dot{\theta}, \dot{\psi})$ defined in the ship-fixed axis system:

$$\begin{cases} \varphi = \dot{\varphi} + \dot{\theta} \cdot \sin\varphi \cdot \tan\theta + \dot{\psi} \cdot \cos\varphi \cdot \tan\theta \\ \theta = \dot{\theta} \cdot \cos\varphi - \dot{\psi} \cdot \sin\varphi \\ \psi = \left(\dot{\theta} \cdot \sin\varphi + \dot{\psi} \cdot \cos\varphi\right) \cdot \sec\theta^2 \end{cases} \tag{2}$$

The position and velocity vectors of the craft's centre of gravity, $\underline{x_0}$ and $\underline{u_0}$ respectively, in the space-fixed axis system are obtained by using a transformation matrix T_0 based on the angular orientation of the craft:

$$\underline{u_0} = T_0 \cdot \underline{U}$$

$$\underline{x_0} = \int_0^t \underline{u_0} \cdot \mathrm{d}t \tag{3}$$

where $\underline{U}$ denotes the ship-fixed velocity vector (u, v, w) and t is time.

These equations of motion form the basis of the simulation program. The differential equations can be solved by means of standard numerical integration techniques. The challenge is to determine the various force components contributing to the right hand side, in particular the force components acting on the vessel. The force and moment vector $\underline{X}$ consists of the components proposed in Eq. 4:

$$\underline{X} = X_p + X_{ap} + X_h \tag{4}$$

where the indices p, ap and h denote the propellers, appendages and hull, respectively. The propeller and appendage forces are based on semi-empirical relations. The propeller forces for instance are obtained from Wageningen B-Series open water characteristics while viscous roll damping is based on the Fast Displacement Ship (FDS) [9] method. The propeller rpm is constant during the simulation. The variations in advance coefficient due to forward speed are taken into account.

The hull forces due to forward speed and waves are based on a time domain panel method with exact forward speed effects. It is a pure time domain method without any frequency domain content like added mass and damping coefficients. It features linear radiation and diffraction forces with non-linear (body-exact) wave excitation and restoring forces. Manoeuvring forces are based on representing the hull as a low aspect ratio lifting surface and a cross-flow drag method. More information can be found in [10].

The selected version of *PANSHIP* accounts for radiation and diffraction forces with reference to the mean submerged geometry at speed while the wave excitation and restoring forces are determined for the instantaneous wetted hull geometry. The boundary conditions on the free surface are linearized, thus the software is not fully non-linear.

The use of the transient free surface Green function allows for accurate predictions for high speed craft, low and moderate speed craft can be dealt with as well. Validations in stern quartering irregular waves were carried out in [11–13] showing a good agreement with model test results.

PANSHIP is mostly used for 6-DoFs seakeeping and manoeuvring analysis: it can deal with different ships typology and multiple vessels at the same time. To achieve these results, complex parameters that have an impact on simulations need to be tuned. Particular attention was paid to tuning of numerical results on measurements collected during model tests carried out in stern quartering waves. Three parameters have been investigated: first, the cross flow drag coefficient along

Author's personal copy

the transversal *y*-direction *Cdy*, to improve the evaluation of the effect of viscous drag. Second, the FDS method was selected as the standard viscous roll damping method in simulations. Third, a deeper analysis was conducted to study the effect of skeg aspect ratio, introducing a characteristic skeg height to enhance the estimation of the lift force exerted by this ship's appendage.

The autopilot is based on a straightforward PD type controller without integrator term. This means that for oblique wave directions the mean heading may deviate from the nominal heading by a small amount limited to a few degrees. The equations used are:

$$\delta = C_{\psi} \cdot \left(x_{i,\mathrm{act}} - x_{i,\mathrm{req}}\right) + D_{\psi} \cdot \left(\dot{x}_{i,\mathrm{act}} - \dot{x}_{i,\mathrm{req}}\right) \tag{5}$$

here δ is the control surface deflection, $x_{i,\mathrm{act}}$ is the actual motion, $x_{i,\mathrm{req}}$ is the required motion value (usually 0) and C_{ψ} and D_{ψ} are the proportional and damping gains, respectively.

As already mentioned, the main quality of a numerical tool, in principle suitable for direct assessment, is to investigate the hydrodynamic problems with a superior level of accuracy. This is the reason why differences in comparison with the second vulnerability criteria are inherently expected. These differences are evident for the hydrodynamic forces computation. Only the Froude–Krylov force, dependent on the incident wave elevation, has been modeled in the surf-riding vulnerability criterion in the framework of SGIS criteria. It is computed with a simplified methodology based on the hull geometry distribution by transverse sections. The numerical software used for the simulations computes, as already mentioned, the instantaneous incident wave forces on the instantaneous wetted surface body considering the irregular sea state wave profile.

3 The investigated units and the selected sea state conditions

Two yachts and a patrol boat with classic spade rudders and twin shaft arrangement have been investigated in this paper; their main dimensions are given in Table 1 together with the investigated wave conditions. The selected units for the applications are limited in length. None of them would successfully fulfill the first vulnerability level of SGIS criteria for the surf riding, which defines the ship as vulnerable if lower than 200 [m] in length. Moreover the two yachts are rather similar in terms of size and the patrol boat is significantly smaller. These features create an interesting domain of investigation in order to compare different assessment tools i.e. numerical simulation and SGIS criterion. A tridimensional view of the yacht 2 hull, modeled within PANSHIP, is shown in Fig. 1. The number of panels selected for the input mesh of yacht vessels has been set between 4000 and 5000; for the patrol boat a number between 3000 and 4000 panels has been used to preserve an equivalent level of discretization, in relation with the difference in length compared to yacht vessels. Differently from the patrol boat, the two yachts are provided with stabilisation fins. In the simulations, fins were considered passive. Specific values of gyration radius i.e. $R_{xx} = 0.38B$ [m] and $R_{yy} = R_{zz} = 0.25L_{PP}$ [m] have been assumed, being these typically associated with the selected hull typologies. The position of the vertical centre of gravity *KG* has been selected between 0.70 and 0.75% of the ship depth *D*, in relation with the specific unit.

The autopilot settings, assumed for all the ships, are the following:

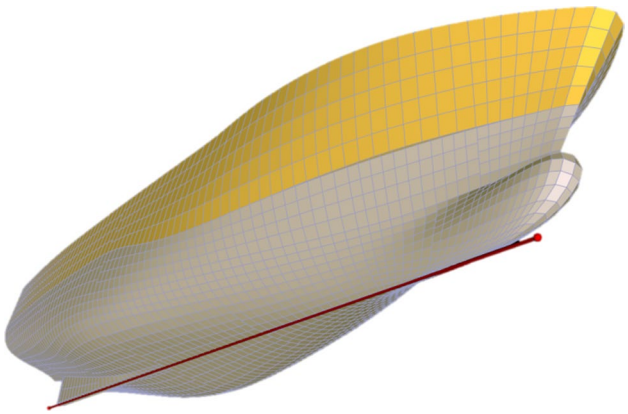

Fig. 1 Tridimensional view of yacht 2 modeled within PANSHIP. Courtesy of Fincantieri

Table 1 Overview of the ship and wave data used in the investigation

Database	Geometry						Speed		Waves	
Type	L_{PP} (m)	B (m)	T (m)	Δ (t)	R_{XX} (m)	$R_{YY} = R_{ZZ}$ (m)	V_S (kn)	Fn (−)	H_S (m)	T_P (s)
Yacht 1	67.60	14.5	4.01	2337.40	5.51	16.90	13.1	0.262	2.03	5.38
							15.1	0.302		
Yacht 2	76.84	14.0	3.70	2190.81	5.32	19.21	13.5	0.253	2.31	5.74
							15.8	0.296		
Patrol Boat	13.00	3.71	Ta = 0.672	13.60	1.41	3.25	12.8	0.583	1.86	5.14
			Tf = 0.762				14.6	0.665		

Author's personal copy

- Rudders maximum angle $\delta_{\max} = 35$ [°];
- Rudders rate of turn $\dot{\delta} = 4$ [°/s];
- Rudder proportional and damping PD gains $C_{\psi} = 3$ [°/°], $D_{\psi} = 6$ [°/(°/s)]

Simulation length was set to 1 h and the other computational parameters have been properly selected in order to standardize the environmental conditions as a function of the ship main dimensions.

An irregular sea state characterized by waves with a peak steepness of $s_p = 0.045$ [−] has been selected [14]. The peak period is then calculated as defined in Eq. 6:

$$T_p = \sqrt{\frac{H_s}{\frac{g}{2\pi} s_p}} \tag{6}$$

where H_S is the significant wave height [m].

The *JONSWAP* sea spectrum with a peak enhancement factor $\gamma = 3.3$ [−] has been selected. Its validation has been carried out in [14, 15]. No spreading function has been taken into account.

To take into account realistic short-term sea state in terms of probability of occurrence, the sea state parameters have been identified according to the Mediterranean and Caribbean scatter diagrams [16]. With this intent, H_S is assumed equal to the 1.3% of L_{PP} for patrol boat and the 3% of L_{PP} for yachts. The wavelength is assumed equal to the vessel length.

Stern quartering seas investigations have been carried out selecting five prevalent wave directions:$\mu = 15, 30, 45, 60, 75$ [°], in accordance with the standard convention that identifies following sea as $\mu = 0$ [°].

Two different forward speeds have been selected for each vessel. The first one refers to the operational speed of the unit. For each ship, another speed has been properly selected, able to guarantee the results reliability and to ensure a standardized number of wave encounters at $\mu = 45$ [°].

3.1 Simulation process

Firstly, from the 3D hull surface, the hull mesh has been generated using a commercial meshing plug-in.

Successively, the mesh has been imported in Panview (application software of Panship) to check the geometry generated by panel distribution above and below the waterline. Then the input file has been prepared: appendages of the vessel (bilge keels, fins, rudders, head-boxes, skeg) have been modelled relying on a 2D rectangular lifting surface, with equivalent surface area and CoG.

After generating the complete mesh file, inclusive of appendages, as a first step, calm water simulations (with CalmWater, application software of Panship) have been performed, in order to find the equilibrium position in calm water at a given forward speed. The equilibrium position is determined in terms of vessel trim and sinkage convergence.

Once the equilibrium position of the vessel at a given speed has been found, panels are redistributed according to the new equilibrium waterline: this process will determine the mean submerged geometry of the vessel for seakeeping purpose.

Finally, simulations in waves have been performed according to the parameters indicated in the previous section: the ship at the relevant equilibrium position and given speed is put in an irregular sea state, characterized by the ζ function generated from the wave spectrum.

The initial transient part of the simulation has not been considered in results computation by the software.

A previous calibration of the software has been carried out with specific attention to ship motions (roll, yaw, CoG-y acceleration). Ad hoc simulations have been performed for yacht 1 and yacht 2 to match available model tests data, with a focus on sensitivity analysis for effects of roll damping, cross flow drag and skeg aspect ratio, obtaining a good general agreement with model tests results. These calibrated parameters have been applied to all the simulations discussed in the present study, as already mentioned in the paragraph describing the numerical tool.

4 Postprocessing of the *PANSHIP* simulation results

4.1 Definition of surf-riding

The assessment for surf-riding has been numerically performed through a post-processing activity focused on the wave elevation $\zeta(t)$, being one of the *PANSHIP* outputs. The wave elevation is defined within the numerical tool as the incident wave elevation of an irregular sea state at the longitudinal position of the centre of gravity. This post-processing activity has been carried out by means of a dedicated MATLAB scripts.

To identify the surf-riding phenomenon, a method based on three specific conditions has been selected. The first condition is related to $\zeta(t)$: when this function assumes a constant value over a selected amount of time, the relative position of the ship with reference to the wave does not change. It means the ship is moving with the wave.

In a surf-riding event, the ship forward speed is accelerated to the wave celerity:

$$V_S(t) = C_w(t) \tag{7}$$

Author's personal copy

Table 2 Definition of surf-riding

Description	Surf-riding
Ship's forward speed	$V_s(t) = \text{const}$
Wave elevation w.r.t. ship's CoG	$\zeta(t) = \text{const}$
Wave elevation derivative	$\dot{\zeta}(t) = 0$

Table 3 Definition of broaching

Description	Broaching
Yaw angle	$\psi(t) \geq 20°$
Rudder angle	$\delta(t) = \delta_{\max}$
Yaw rate $\dot{\psi}(t)$ and Yaw acceleration $\ddot{\psi}(t)$ have the same sign	

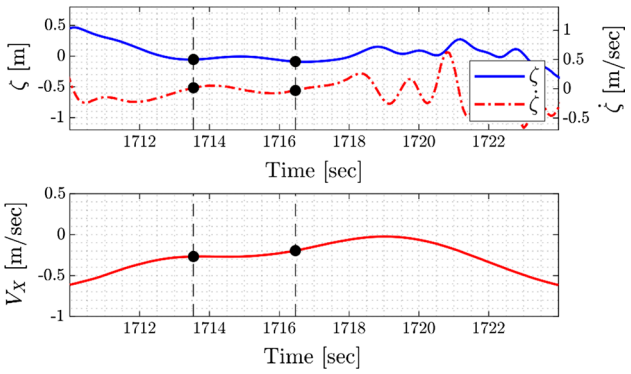

Fig. 2 Example of a surf-riding event recorded in a simulation

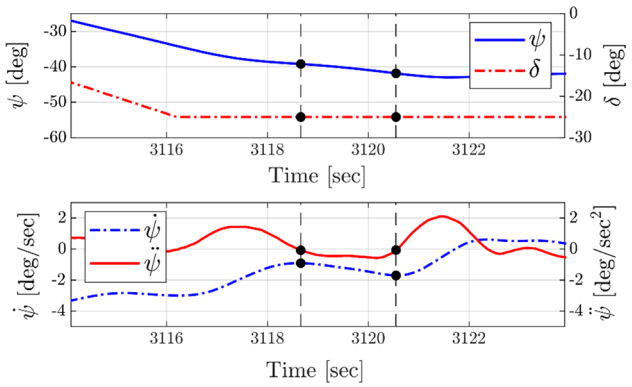

Fig. 3 Example of broaching event recorded in a simulation

where $V_s(t)$ is the ship's forward speed and $C_w(t)$ is the instantaneous speed of the considered wave crest.

When $\zeta(t)$ is constant, it is possible to assume that the condition proposed in Eq. 7 is automatically achieved. Once the ship is accelerated to the wave celerity, the ship forward speed will not vary in this condition, thus:

$$V_S(t) = \text{const}. \tag{8}$$

A further condition related to the function derivative $\dot{\zeta}(t)$ is considered as well, for numerical reasons. In Table 2 an overview of these conditions can be found.

Within the post-processing tool, the user can select the time length of the surf-riding event t_{sr} to be investigated. A general output in terms of time history is presented in Fig. 2. The surf-riding event is within the range between the black dots and it has been identified according to the conditions expressed in Table 2.

In Fig. 2, the function ζ (t) and its derivative $\dot{\zeta}(t)$ are shown in the upper graph, while in the lower graph the forward speed variation with reference to the mean value $V_x = V_S(t) - V_{\text{mean}}$ is reported. $V_S(t)$ is the instantaneous ship forward speed, while V_{mean} is the ship mean speed in irregular sea during the whole simulation time.

4.2 Definition of broaching

This paper adopts the method defined by [17] to assess the broaching event. Three conditions, to comply with at the same time, are suggested in order to identify the broaching event. They are summarized in Table 3.

These conditions well represent the typical scenario of broaching, defined as follows: when the ship's heading angle in a seaway condition exceed a threshold value, the rudder moves to its maximum angle in order to counteract it. However, if yaw rate and yaw acceleration have the same sign, it means that the heading angle is continuously increasing despite the maximum steering effort. This situation may lead to an uncontrollable ship turning and perhaps capsizing.

To identify broaching events from the numerical simulations, conditions in Table 3 have been implemented in a MATLAB post-processing tool similar to the one developed for the surf-riding phenomenon. In Fig. 3 a general output of broaching is presented. The upper graph shows the rudder angle $\delta(t)$ and the yaw angle $\psi(t)$; the maximum rudder angle in this simulation has been set equal to 25 [°]. It is possible to see that the yaw angle exceeds the threshold value fixed in Table 3. The lower graph shows the yaw rate $\dot{\psi}(t)$ and the yaw acceleration $\ddot{\psi}(t)$. In the represented time range, the yaw rate is always negative except after $t = 3122$ [s], therefore the yaw acceleration, definitely more variable, is the governing parameter to comply or not with the broaching conditions of existence.

Author's personal copy

5 IMO SGISc surf-riding/broaching second vulnerability level criterion

In this paper, specific attention is given to the second level of vulnerability criteria for the surf-riding stability failure mode, since the first level criterion is very simple and it only considers the ship length and the relevant Froude number.

With reference to the second vulnerability level procedure, the C index is calculated as defined in Eq. 9. A ship is considered not vulnerable to surf-riding phenomenon if the C index is lower than the IMO threshold value $R_{SR} = 0.005[-]$.

$$C = \sum_{H_s}\sum_{T_z}\left(W2(H_s,T_z)\cdot\sum_{i=1}^{N_\lambda}\sum_{j=1}^{N_a}W_{i,j}\cdot C2_{i,j}\right) \tag{9}$$

The C index represents a long-term probability expressed as the weighted sum of the short-term stability failure index over all the sea states defined by H_S and T_Z. Each single short-term index $C2_{i,j}$ is multiplied by both a long term occurrence weight $W2(H_s,T_z)$ and a statistical weight W_{ij}, defined as a function of wave/ship length ratio r_i and wave steepness s_j. The short-term index could be 0 or 1, depending on the relationship between the ship forward speed u and a critical ship forward speed $u_{cr,ij}$.

The critical ship forward speed $u_{cr,ij}$ is defined as the threshold between surging and surf-riding phenomena. This threshold is obtained by the determination of the critical propeller revolutions $n_{cr,ij}$ by means of an appropriate iteration processes defined below. The whole procedure to compute the long-term index C can be found in details in [1, 18].

In order to calculate the C index for the selected units described in Table 1, the following input data are needed:

- The total resistance curve $R_t(V_s)$, necessary to compute hull resistance regression coefficient $r_0, r_1, \ldots, r_5$. To obtain this curve, resistance model test reports have been used when available, otherwise the resistance curve has been obtained through a numerical method (*PANSHIP* CalmWater simulations);
- The open water propeller curve $K_t(J)$, necessary to compute propeller curve regression coefficient $\kappa_0, \kappa_1, \kappa_2$;
- Ship's sectional submerged area, sectional draught and sectional position with respect of ship's longitudinal position of CoG measured at design draught. This data are required to calculate the effective wave slope coefficient by a simplified formulation defined by the criterion.

Then, it is necessary to iteratively solve Eq. 10 to determine the critical revolutions of the propeller n_{cr}:

$$n_{cr} = 2\pi\frac{T_e(c_i;n_{cr}) - R(c_i)}{f_{ij}} + 8a_0 n_{cr} + 8a_1 - 4\pi a_2 + \frac{64}{3}a_3 - 12\pi a_4 + \frac{1024}{15}a_5 = 0 \tag{10}$$

where $a_0, a_1, \ldots, a_5$ are coefficients described in [1], c_i is the considered wave celerity, f_{ij} is the amplitude of wave surging force, $R(c_i)$ is the hull resistance measured at the wave celerity and $T_e(c_i;n_{cr})$ is the thrust as a function of n_{cr}, provided by the propellers at a speed equal to the wave celerity. A step of $\Delta n_{cr} = 0.001$ [rps] has been selected to iteratively solve Eq. 10. Once n_{cr} has been calculated, it is necessary to iteratively solve Eq. 11 in order to find the critical ship forward speed u_{cr} to:

$$T_e(n_{cr};u_{cr}) - R(u_{cr}) = 0 \tag{11}$$

In this case, a step of $\Delta u_{cr} = 0.01$ [m/s] has been adopted.

6 Calculation and remarks

The C indexes obtained for yacht 1, yacht 2 and patrol boat are presented in Fig. 4. On the horizontal axis the Fn number is reported and on the vertical axis the C index is presented in a logarithmic scale. The red horizontal line stands for the IMO threshold value R_{SR}, a ship is declared vulnerable to surf-riding when C index is greater than that threshold.

The C indexes are reported in a range of Fn = 0.2 to 0.4 with a step of ΔFn = 0.01. At lower Fn number, yacht 2 seems less vulnerable than yacht 1 but at higher speed the situation is reversed. The Fn safe zone of yacht 1 decreases

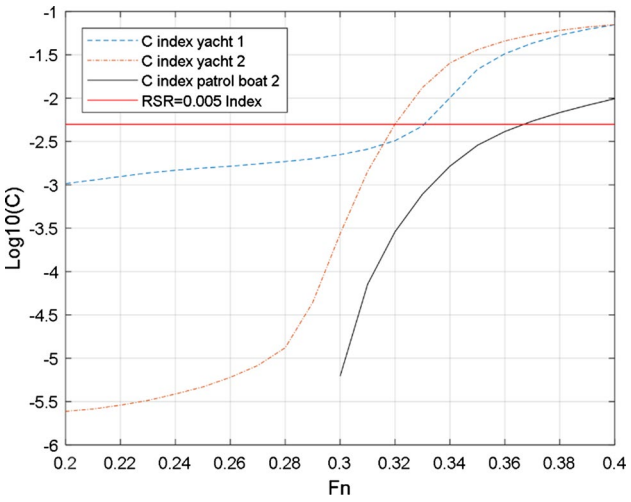

Fig. 4 C indexes as a function of Fn for yacht 1, yacht 2 and patrol boat

Author's personal copy

sharply for values greater than 0.28, over passing the threshold at Fn = 0.32. The patrol boat appears to be the less vulnerable vessel when observing the problem in terms of Froude number, it overcomes the threshold for Fn greater than 0.36. As a recap, the critical Froude numbers for each ship are reported in Table 4.

According to the philosophy that inspired the SGIS criteria, first levels should be more conservative than second levels. Since by the first level a ship is considered vulnerable when her Froude number is greater than 0.3, the outcomes of second level analysis point out that the allowed Froude numbers for each unit are greater than those permitted by the first level. It means that the consistency between levels is verified, however the increments in terms of speed allowed by the second level are not so remarkable.

In the numerical calculations, values of representative speed of typical operational conditions have been selected for the investigated units. As a consequence, the two yachts have been assessed with Fn lower than the critical ones (expressed in Table 4) and the patrol boat with a Froude number that is higher. The numerical assessment has been carried out with reference to the environmental condition as described in the third paragraph.

It is worth mentioning that it is not so straightforward to guarantee the equivalence of environmental conditions between the numerical calculations and second vulnerability criterion and this could in principle affect the comparison of relevant results. *C* index is build up weighting the effect of a single regular following wave with parameters identified in terms of steepness and wavelength to ship length ratio. Differently, the proposed numerical assessment is based on an irregular sea state for which it is not possible to follow the same procedure in terms of ship/wave interaction to identify a surf-riding event. The methodology based on numerical results is formulated with a different physical concept, i.e. it is not strictly derived from a stability equilibrium analysis but just from a time-domain analysis of the wave elevation and the ship's forward speed mutual interaction.

Moreover in this case, the North Atlantic scatter diagram has been considered in the second vulnerability level assessment while the Mediterranean and Caribbean areas have been selected for the numerical calculation, since more realistic for such units.

In the post-processing of the output, attention is focused on the time range during which all the conditions in Table 2 are fulfilled, i.e. the ship is expressing a surf-riding behaviour. Such time parameter is named t_{sr} and it is measured in seconds. During a simulation, it is possible to identify several t_{sr} time periods where the conditions of Table 2 are simultaneously true. For the investigation, the selection among them of the longest one $t_{sr,longest}$ has been considered useful to realistically identify a surf-riding event.

Then, in line with the vulnerability criteria, an arbitrary threshold needs to be defined t_{thrs} in order to process the parameter $t_{sr,longest}$. In particular, when $t_{sr,longest} > t_{thrs}$ the ship is considered vulnerable to surf-riding phenomenon. Table 5 shows the final comparison between the SGIS criterion Level 2 surf-riding and the outcome of the direct calculations by the numerical time domain tool considering the above mentioned threshold of $t_{thrs} = 5$ [s].

The "Longest surf-riding event" and "Numerical surf-riding" columns are directly linked: a vessel is considered vulnerable to surf-riding by the proposed numerical method if the longest surf-riding event is longer than the selected threshold. It is interesting to notice that time frames $t_{sr,longest}$ of yacht 2 are longer than those of yacht 1.

As concerns broaching failure mode, results show that no events have been found for the chosen sea state. We deem that this is due to the selected autopilot characteristics; in every simulation, the yaw angle did not overpass the assumed threshold $\psi = 20$ [°]. In light of these results, a direct connection between the surf-riding and broaching-to events cannot be found.

Table 4 Critical Fn numbers for which $C > 0.005$

Database	Critical Fn
Yacht 1	0.330
Yacht 2	0.320
Patrol Boat	0.376

Table 5 Comparison between numerical analysis and SGIS criterion results, $t_{thsr} = 5$ (s)

	Fn	V_S (m/s)	Longest surf-riding event $t_{sr,longest}$ (s)	Numerical surf-riding	Numerical broaching	SGISc surf-riding
Yacht 1	0.26	6.73	7	V	NV	NV
	0.30	7.76	5	V	NV	NV
Yacht 2	0.26	6.94	8	V	NV	NV
	0.30	8.12	14	V	NV	NV
Patrol boat	0.58	6.58	6.5	V	NV	V
	0.66	7.50	4.5	NV	NV	V

V Vulnerable, *NV* not vulnerable

Author's personal copy

Concerning the comparison between numerical simulation and vulnerability level analysis, a poor agreement of the results for yacht 1 and yacht 2 is shown . The numerical tool reveals surf-riding events while the SGIS criterion declares these vessels as not vulnerable for the assessed speed; the *C* index for both vessels is surpassed only at higher values of Fn. On the contrary, the two methods agree for one speed in the patrol boat assessment. The numerical tool declares the ship vulnerable at Fn = 0.58 and not vulnerable at Fn = 0.66 while the SGIS criterion considers the unit vulnerable for Fn greater than 0.376.

To understand the influence of the threshold t_{thrs}, the same analysis has been carried out considering $t_{\text{thrs}} = 10$ [s]. This value is the lower boundary surf-riding event duration assumed in [19]. The obtained results are shown in Table 6.

Outcomes show a better agreement between the numerical analysis and the second vulnerability level criterion: for yacht vessels a good agreement has been found between the two methods. Both the vulnerability level and the numerical simulation judge the two yachts not vulnerable for both speeds, except for the highest speed of yacht 2 where the numerical simulation considers the vessel as vulnerable. For the patrol boat, the numerical assessment does not reveal any vulnerability in contrast to the SGIS criterion assessment. These results found second vulnerability level to be conservative for this vessel type under the proposed conditions and assumptions, and this is in line with the philosophy at the basis of the SGIS criteria.

As already mentioned, the main focus of this investigation is to compare different assessment tools. It is evident how the consistency between the numerical analysis and the SGIS criterion strongly depends on the threshold of the longest surf-riding event. On the other side, in the perspective to compare instead the performance of vessels with different sizes, an interesting analysis would be to understand the influence of the vessel size on the surf riding event.

It should be noted that the numerical assessment applied in this study does not completely fulfill the methodology defined in the IMO *Specification of Direct Stability Assessment procedures* [1]. Three different assessment are to be implemented to carry out the Direct Stability Assessment (DSA) in relation with the environmental condition of the simulation. The three procedures are the *Full probabilistic assessment*, the *Assessment in design situations using probabilistic criteria* and the *Assessment in design situations using deterministic criteria*.

In the first procedure the simulation of all the relevant sea states, wave directions and ship forward speed is requested; the criterion used is the weighted average of the mean long-term failure rate.

The second and third procedures, i.e. Assessment in design situations, using either the probabilistic or the deterministic criteria, consider a limited combination of ship speeds, wave directions, significant wave heights and mean zero-up crossing periods. In the probabilistic assessments, the elapsed time from the starting time of the simulation up to the first failure event T_{fail} is considered to calculate the stability failure rate r as defined in Eq. 12:

$$r = 1/\sum_{i} T_{\text{fail},\,i} \tag{12}$$

The deterministic procedure, instead, takes in to account the mean 3-h maximum roll amplitude over a fixed time period. Further details about the IMO post-processing procedures can be found in Annex 1 of [1].

The differences in the post-processing activity may play a significant role when reasoning about consistency problems with the vulnerability levels.

7 Conclusions

In this paper, numerical simulations have been carried out and analysed to capture the likelihood of a surf-riding and/or broaching event in stern quartering seas. The numerical software was tuned with experimental data and selected sea state conditions, autopilot settings and ship's characteristics have been identified to perform simulations.

Table 6 Comparison between numerical analysis tool and IMO SGIS criterion results, $t_{\text{thsr}} = 10$ (s)

	Fn	V_S (m/sec)	Longest surf-riding event $t_{\text{sr,longest}}$ (s)	Numerical surf-riding	Numerical broaching	SGISc surf-riding
Yacht 1	0.26	6.73	7	NV	NV	NV
	0.30	7.76	5	NV	NV	NV
Yacht 2	0.26	6.94	8	NV	NV	NV
	0.30	8.12	14	V	NV	NV
Patrol boat	0.58	6.58	6.5	NV	NV	V
	0.66	7.50	4.5	NV	NV	V

V Vulnerable, *NV* not vulnerable

Author's personal copy

Results relevant to a set of three ships, two yachts and a patrol boat, have been presented and compared with second vulnerability level of surf-riding criterion. In the following, considerations about such outcomes are given, from both a conceptual and practical point of view:

- The SGIS second level vulnerability criterion for surf-riding/broaching is rigorously based on surf-riding events, no attention is effectively posed on broaching dynamics. On the contrary a numerical assessment can in principle provide an analysis of broaching taking into account physical aspects of this phenomenon.
- For evaluations based on the numerical tool, two independent numerical post-processing approaches have been considered: one able to identify surf-riding events and another able to identify broaching events. Nevertheless the obtained results cannot show the link between the two phenomena, because no broaching event has been found during the simulations even in cases where the surf-riding event has been identified.
- In the SGIS criterion, the *C* index is calculated weighting the effect of single regular following wave identified by the regulation with reference to the ship length. On the contrary, the proposed numerical assessment is based on an irregular sea state for which it is not possible to follow the same SGIS criterion procedure for the surf-riding event identification.
- The comparability issue between the two assessment tools is also evident for the hydrodynamic forces computation. In SGIS criterion, these forces are reduced to the sole Froude-Krylov force dependent on the incident wave elevation and simplified hull geometry. On the contrary, to perform numerical simulations, the software computes the incident wave forces on the instantaneous wetted surface body, considering the irregular sea state wave profile. The radiation and diffraction forces are computed on the average wetted surface body. In conclusions, as put in evidence in several occasions, the SGIS criterion and numerical assessment methods present different levels of accuracy that have an impact on the safety margins implemented in the standards.
- The consistency between the numerical analysis and the SGIS criterion strongly depends on the threshold of the longest surf-riding event. Experimental data could be of key importance to identify a proper threshold time to detect the vessel vulnerability to surf-riding in numerical analysis approach.

References

1. SDC 6/WP.6. (2019) Finalization of second generation intact stability criteria. In: Report of the expert's group on intact stability. International Maritime Organization, London
2. Umeda N, Matsuda A, Hamamoto M, Suzuki S (1999) Stability assessment for intact ships in the light of model experiments. J Mar Sci Technol 45(4):45–57
3. Umeda N, Hashimoto H, Matsuda A (2003) Broaching prediction in the light of an enhanced mathematical model, with higher order terms taken into account. J Mar Sci Technol 145(7):145–155
4. Spyrou K (1996) Dynamic instability in quartering seas: the behaviour of a ship during broaching. J Ship Res 40(1):46–59
5. Spyrou K (1995) Surf-riding, yaw instability and large heeling of ships in following/quartering waves. Shiffstechnik 42(2):103–112
6. Spyrou K (1995) Surf-riding and oscillations of a ship in quartering seas. J Mar Sci Technol 1:24–36
7. Belenky V, Bassler C, Spyrou K (2011) Development of second generation intact stability criteria. In: Hydromechanics department report. Naval Warfare Center Carderock Division, Carderock
8. De Jong P (2011) Seakeeping behaviour of high speed ships: an experimental and numerical study. Unpublished Doctoral Dissertation. University of Technology, Delft
9. Blok JJ, Aalbers AB (1991) Roll damping due to lift effects on high speed monohulls. In: Proceedings of the 1st international conference on fast sea transportation. Trondheim
10. van Walree F, Sgarioto D, Turner TG (2016) Validation of a time domain panel code for prediction of impulsive loads on high speed ships. In: Proceedings of the 31st ONR symposium on naval hydrodynamics. Monterey
11. van Walree F (2002) Development, validation and application of a time domain seakeeping method for high speed craft with a ride control system. In: Proceeding of the 24th symposium on naval hydrodynamics. Fukuoka
12. van Walree F, De Jong P (2011) Validation of a time domain panel code for high speed craft operating in stern quartering seas. In: Proceedings of the 11th international conference on fast sea transportation. Honolulu
13. van Walree F, Verboom E (2015) Validation of time domain panel codes for prediction of large amplitude motions of ships. In: Proceedings of the 12th international conference on the stability of ships and ocean vehicles. Glasgow
14. Arena F, Guedes Soares C, Petrova P (2010) Theoretical analysis of average wave steepness related to peak period or to mean period. In: Proceedings of the 29th international conference on ocean, offshore and arctic engineering. Shanghai, pp 1–3
15. Bitner-Gregersenm E, Guedes Soares C, Silvestre A (1998) On the average wave steepness. In: Proceedings of the conference ocean wave kinematics, dynamics, and loads on structures. Houston, pp 513–520
16. European Centre for Medium-Range Weather Forecasts (2019) Forecasts datasets ERA-Interim. www.ecmwf.int/en/forecasts/datasets/reanalysis-datasets/era-interim
17. Renilson M, Tuite A (1998) Broaching-to—a proposed definition and analysis method. In Proceedings of the 25th American towing tank conference. Iowa
18. SDC 4/5/1 (2016) Finalization of second generation intact stability criteria. *In:* Report of the correspondence group (submitted by Japan). International Maritime Organization, London
19. De Jong P, Renilson M, Walree F (2015) The effect of ship speed, heading angle and wave steepness on the likelihood of broaching-to in astern quartering seas. In: Proceedings of the 12th international conference on the stability of ships and ocean vehicles. Glasgow

Publisher's Note Springer Nature remains neutral with regard to jurisdictional claims in published maps and institutional affiliations.